Pre-Steady-State Transition-State Analysis of the Hydrolytic Reaction Catalyzed by Purine Nucleoside Phosphorylase†

Paul C. Kline‡ and Vern L. Schramm*

Department of Biochemistry, Albert Einstein College of Medicine, 1300 Morris Park Avenue, Bronx, New York 10461

Received June 24, 1994; Revised Manuscript Received November 1, 1994®

ABSTRACT: The slow hydrolytic reaction catalyzed by calf spleen purine nucleoside phosphorylase [Kline, P. C., & Schramm, V. L. (1992) *Biochemistry 31*, 5964−5973] has been investigated using pre-steady-state kinetic isotope effects and solvolysis studies. The stoichiometric reaction between enzyme and inosine forms 1 mol of free ribose per trimer of purine nucleoside phosphorylase and a tightly bound complex of enzyme and hypoxanthine. The experimental kinetic isotope effects from [1′-^{3}H]-, [2′-^{3}H]-, [4′-^{3}H]-, [5′-^{3}H]-, [1′-^{14}C]-, and [9-^{15}N]inosine are 1.151 ± 0.004, 1.145 ± 0.003, 1.006 ± 0.004, 1.028 ± 0.005, 1.045 ± 0.005, and 1.000 ± 0.005, respectively, for the pre-steady-state conditions. Substrate trapping experiments demonstrated that there is no detectable forward commitment to catalysis for inosine hydrolysis. In contrast, bound inosine is 2.1 times more likely to form product than to dissociate when the enzyme−inosine complex is exposed to saturating PO_4. The lack of an observed 9-^{15}N isotope effect is consistent with an internal equilibrium between enzyme−inosine and the enzyme−hypoxanthine−ribose complex in which N9 of hypoxanthine is protonated. The equilibrium occurs as a consequence of slow product release and tightly bound hypoxanthine ($K_d = 1.3 \times 10^{-12}$ M). This internal equilibrium has a minimal effect on the intrinsic kinetic isotope effects from ribose since equilibrium isotope effects for conversion of inosine to ribose are near unity. When the single-turnover hydrolytic reaction was accomplished in 20% methanol, approximately 85% of the product sugar was 1-methylribose. Under these conditions, the anion-binding pocket fills with solvent which competes for the oxocarbenium ion of inosine formed at the transition state. In the presence of arsenate, no methanolysis of inosine occurs [Kline, P. C., & Schramm, V. L. (1993) *Biochemistry 32*, 13212−13219]. The results define a transition state with oxocarbenium ion character and weak participation of the attacking solvent nucleophile. Electrostatic potential surfaces of the transition states indicate that arsenate anion is more effective in neutralizing the oxocarbenium ion than is H_2O.

Purine nucleoside phosphorylase (EC 2.4.2.1) from calf spleen cleaves the C−N bond of inosine, guanosine, or their 2′-deoxynucleosides according to the reaction:

purine (deoxy)nucleoside + $P_i \rightleftarrows$
purine base + α-D-(deoxy)ribose 1-phosphate (1)

Reaction 1 has been shown to occur with inversion of configuration at the anomeric carbon of ribose (Parks & Agarwal, 1972). Arsenate can replace phosphate in the reaction, with the unstable α-D-ribose 1-arsenate hydrolyzing to give ribose and arsenate. Steady-state kinetics have been reported to conform to an ordered mechanism with nucleoside binding prior to phosphate for the calf spleen and human erythrocyte enzymes (Kim et al., 1968; Krenitsky, 1967) or to an ordered mechanism with phosphate binding first (Porter, 1992). Substrate-trapping experiments are consistent with a random addition of inosine and arsenate (Kline & Schramm, 1993).

In addition to phosphorolysis and arsenolysis reactions, the enzyme is capable of catalyzing the slow hydrolytic cleavage of the C−N glycosidic bond of inosine or guanosine (Figure 1). The hydrolysis of inosine is accompanied by the formation of a tightly bound complex containing a trimer of purine nucleoside phosphorylase subunits and a single hypoxanthine. The pre-steady-state kinetic mechanism of the hydrolytic reaction includes a burst of product formation equal to a single turnover at one of the three symmetric catalytic sites followed by a slow steady-state reaction in which the rate-determining step is release of hypoxanthine (Kline & Schramm, 1992).

Transition states for several *N*-glycosidic enzymes have been studied using multiple kinetic isotope effects. Nucleoside hydrolase, native and mutant AMP nucleosidases, and the arsenolysis reaction catalyzed by purine nucleoside phosphorylase (Horenstein et al., 1991; Mentch et al., 1987; Parkin et al., 1991; Kline & Schramm, 1993) were found to contain similar transition states in which the C−N glycosidic bond is extensively broken, substantial oxocarbenium ion character exists on the ribosyl group, low bond order is present to the attacking (H_2O or arsenate) nucleophile, and the leaving group is N7-protonated. In both the arsenolysis reaction catalyzed by purine nucleoside phosphorylase and the hydrolytic reaction catalyzed by nucleoside hydrolase, the transition state is early, with the preassociated water or oxygen nucleophile situated 3 Å from C1′ of ribose at the transition state. This distance is considerably shorter than the 4.2 Å between the nearest sulfate oxygen and C1′

† This work was supported by Research Grant GM41916 from the National Institutes of Health.

* Address correspondence to this author [telephone (718) 430-2813; FAX (718) 892-0703].

‡ Current address: Department of Chemistry and Physics, Middle Tennessee State University, Murfreesboro, TN 37132.

® Abstract published in *Advance ACS Abstracts,* January 1, 1995.

0006-2960/95/0434-1153$09.00/0

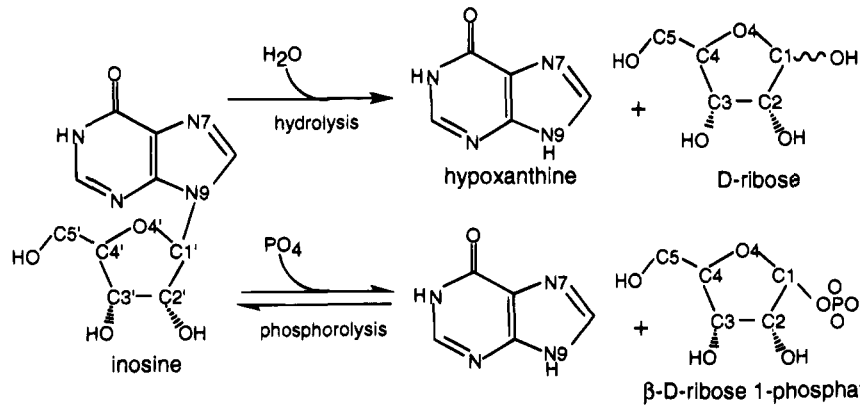

FIGURE 1: Inosine with atomic numbering at the sites labeled for kinetic isotope effects and the reactions for both the hydrolytic and phosphorolysis reactions.

observed in the X-ray crystal structure of purine nucleoside phosphorylase with bound 9-deazainosine and the sulfate in the presumptive anionic site (Ealick et al., 1990).[1] Considerable reaction-coordinate motion is required to move the ribosyl group toward the bound anionic nucleophile before the transition state is achieved (Kline & Schramm, 1993).

Interpretation of the kinetic isotope effects for the arsenolysis reaction of purine nucleoside phosphorylase was complicated by a commitment factor which caused a fraction of bound inosine to be converted to product without being equilibrated with unbound inosine (Kline & Schramm, 1993). The discovery of the slow hydrolytic reaction of purine nucleoside phosphorylase permits the measurement of kinetic isotope effects resulting from a single catalytic turnover. Since hydrolysis is 10^{-4} the rate of arsenolysis, glycosidic bond hydrolysis is more likely to dominate the V_{max}/K_m kinetic isotope effects and therefore provide intrinsic values. Intrinsic kinetic isotope effects can be used to establish the physical properties of the enzymic transition state (Mentch et al., 1987; Horenstein et al., 1991; Horenstein & Schramm, 1993; Kline & Schramm, 1993). Comparison of the transition states for the hydrolytic and arsenolysis reactions of purine nucleoside phosphorylase provides an opportunity to determine the role of the nucleophile in establishing the position of the transition state in the reaction coordinate. This study reports the transition-state structure for the single-turnover hydrolytic reaction of purine nucleoside phosphorylase based on commitment studies, multiple kinetic isotope effects, and bond-energy bond-order vibrational analysis. The results represent the first complete enzymatic transition-state structure which has been established based on pre-steady-state kinetic measurements.

EXPERIMENTAL PROCEDURES

Materials

Purine nucleoside phosphorylase (calf spleen) in 3.2 M ammonium sulfate was purchased from Sigma Chemical Co. The enzyme was desalted on a Sephadex G-25 column eluted with 50 mM triethanolamine hydrochloride, pH 7.5, containing 1 mM dithiothreitol. The desalted enzyme was stored at 4 °C and used within 72 h. Denaturing polyacrylamide gel electrophoresis established that the enzyme was >95% of the total protein in all preparations used for these experiments. Adenosine deaminase, alkaline phosphatase, labeled riboses, and glucoses were purchased from Sigma Chemical Co. Sephadex G-25 was purchased from Pharmacia.

Labeled Nucleosides. Radiolabeled inosines were prepared from the enzymatic conversion of labeled AMP's to inosine using alkaline phosphatase and adenosine deaminase as previously described (Horenstein et al., 1991). The labeled AMP's were prepared from labeled sugar precursors using a combined chemical and enzymatic synthesis (Parkin et al., 1984).

Methods

Substrate Specificity of Calf Spleen Purine Nucleoside Phosphorylase for Adenosine. Reaction mixtures were prepared containing 50 mM triethanolamine hydrochloride, pH 7.5, 50 mM sodium arsenate, and 1 mM adenosine. (*R*)-Coformycin (10 μM) was added to one mixture, and the reactions were initiated by addition of 1 μM purine nucleoside phosphorylase based on the trimer molecular weight of 84 000. The products of the reaction were monitored by reverse-phase HPLC using a Waters μBondapak C_{18} column eluted with 5% MeOH in 5 mM ammonium acetate, pH 5.

Measurement of Pre-Steady-State, Hydrolytic Kinetic Isotope Effects. Purine nucleoside phosphorylase has been previoulsy demonstrated to catalyze third-the-sites reactivity for inosine hydrolysis in the absence of phosphate (Kline & Schramm, 1992). This study demonstrated that 1 mol of tightly bound hypoxanthine and 1 mol of free ribose were formed from 1 mol of trimer purine nucleoside phosphorylase under a wide range of initial concentrations of enzyme and inosine. These studies clearly eliminated the possibility of a contaminant being responsible for the hydrolytic reaction. The same enzyme preparations and controls were used in this work to ensure that pre-steady-state conditions of inosine hydrolysis were being observed. Kinetic isotope effects were measured using the competitive radiolabeled method (Dahlquist et al., 1969; Parkin & Schramm, 1987). The kinetic isotope effect was calculated from the change in the ratio of the natural abundance to the isotopically labeled products of the reaction after approximately 20% of the substrate was converted to products. The original ratios of $^3H/^{14}C$ in the labeled inosines were determined from the $^3H/^{14}C$ isotopic ratio in ribose following complete conversion of inosine to ribose. Insoine with ^{15}N in the *N*-glycosidic bond contained

[1] The coordinates were provided by Dr. Steven Ealick, Cornell University.

a radioactive ^{14}C label at the remote 5′-position as an indicator for the presence of ^{15}N. Reaction mixtures (1 mL) consisted of 100 μM inosine with the desired radiolabels, 50 mM triethanolamine hydrochloride, pH 7.5, and 20 μM purine nucleoside phosphorylase. Reactions were incubated for 10 min (one turnover), and the reaction was quenched by the addition of 100 μL of 1 N HCl. The fractional conversion of inosine to hypoxanthine was established in kinetic isotope effect experiments from the radioactivity in aliquots of the reaction mixture before and after chromatography on cellulose−charcoal. Unreacted inosine is quantitatively retained on charcoal, while the product ribose is eluted [see below and Parkin et al. (1984)].

Reaction mixtures for the complete conversion of labeled inosines to hypoxanthine and ribose consisted of 100 μM inosine with the desired radiolabels and 50 mM triethanolamine hydrochloride, pH 7.5. Complete conversion to products was achieved with excess nucleoside hydrolase (Parkin et al., 1991). Reaction progress was monitored by the ratios of inosine and hypoxanthine peaks on HPLC. Reactions were stopped by the addition of 100 μL of 1 N HCl.

Charcoal−cellulose columns (1:4 dry weight) containing 1.5 mL of packed bed were prepared in Pasteur pipets and loaded with 300 μL of the reaction mixtures and eluted with 100 mM ribose. Fractions of 500 μL were collected directly into scintillation vials, and 500 μL of water was added, followed by 9 mL of scintillation fluid. The samples were counted for six to ten cycles of 10 min each to determine the $^{3}H/^{14}C$ ratio of ribose in the partial and complete conversion of inosine to hypoxanthine and ribose. The observed kinetic isotope effect was corrected for the percent hydrolysis according to eq 2 (Bigeleisen & Wolfsberg, 1958).

$$\text{kinetic isotope effect} = \frac{\ln[1 - (\text{observed KIE}) \times (\text{fraction hydrolyzed})]}{\ln[1 - \text{fraction hydrolyzed}]} \quad (2)$$

Because there was a significant kinetic isotope effect from [5′-^{3}H]inosine, the kinetic isotope effects with [1′-^{14}C]inosine and [9-^{15}N]inosine were also corrected for the [5′-^{3}H]inosine kinetic isotope effect.

Multiple-Turnover Hydrolytic Kinetic Isotope Effects. Kinetic isotope effects were also determined under multiple turnover conditions for the hydrolytic reaction of purine nucleoside phosphorylase by allowing the reaction to proceed for 10 turnovers. Under these conditions, the enzyme concentration was 30 μM, and total inosine was 1000 μM. Samples were incubated for 6 h to achieve the 10 turnovers and processed as described above.

Equilibrium Kinetic Isotope Effects. A mixture of [1′-^{3}H]inosine + [5′-^{14}C]inosine with carrier inosine (800 μM), 5 mM phosphate, and 6 μM purine nucleoside phosphorylase in 50 mM triethanolamine hydrochloride, pH 7.5, was incubated for 3 h at 30 °C to achieve equilibrium. The reaction was terminated with 0.1 M HCl, and the resulting ribose and ribose 1-PO_4 were isolated by charcoal column chromatography eluted with 10 mM ribose 5-PO_4 or 100 mM ribose. The $^{3}H/^{14}C$ ratio was established by scintillation counting.

Commitment to Catalysis. Isotope-trapping experiments used the pulse−chase method described by Rose (1980). For the hydrolytic reaction, 30 μM purine nucleoside phosphorylase (final concentration) was added to a solution containing 400 μM [8-^{14}C]inosine in 50 mM triethanolamine, pH 7.5 (total volume 20 μL). The reaction mixture was incubated for 10 s. No product is formed during the first 10 s under these conditions. A 1-mL chase solution containing 5 mM inosine in 50 mM triethanolamine, pH 7.5, was added at 10 s. The reaction mixtures were incubated to permit 5−10 turnovers and quenched by the addition of 100 μL of 1 N HCl. The reaction mixtures were analyzed for labeled hypoxanthine and inosine using HPLC with a Waters C_{18} μBondapak column (0.4 × 25 cm) eluted with 5% MeOH in water at 1 mL/min. Fractions were collected, and the radioactivity in product and substrate was determined by liquid scintillation counting. Background rates of hydrolysis were determined in control experiments by addition of enzyme to the mixture of [8-^{14}C]inosine and unlabeled inosine in the 1-mL chase solution. The amount of labeled hypoxanthine formed in the control experiment was subtracted from the amount of hypoxanthine formed in the trapping experiment.

The commitment to catalysis for phosphorolysis was determined by isotope trapping to determine whether 10 s is sufficient for enzyme to bind inosine in the absence of anion nucleophile. A 20-μL reaction mixture containing 400 μM [8-^{14}C]inosine in 50 mM triethanolamine, pH 7.5, was made 30 μM in purine nucleoside phosphorylase. The reaction was incubated for 10 s, followed by rapid dilution with 1 mL of a reaction mixture containing 5 mM inosine and variable concentrations of phosphate (100, 125, 200, 2000, and 4000 μM) in the same buffer. After 15 s (sufficient for 5−20 turnovers depending on PO_4 concentration) the reaction was quenched with acid and analyzed as described above. Controls for the conversion of labeled inosine to product following addition of excess inosine and PO_4 combined the labeled and unlabeled inosines and PO_4 in a 1-mL reaction mixture. Enzyme was added, the mixture was incubated for 15 s, and the amount of labeled hypoxanthine formed was subtracted from the amount of labeled hypoxanthine formed in the trapping experiment.

Methanolysis of Inosine. A reaction mixture (1 mL) consisting of 50 mM triethanolamine hydrochloride, 100 μM inosine, [1′-^{3}H]inosine (300 000 cpm), and 20 μM purine nucleoside phosphorylase in 20% methanol was incubated at 30 °C for 15 min. The reaction mixture was then chromatographed on a reverse-phase C_{18} HPLC column to remove unreacted inosine. The column was eluted with 5% methanol in distilled water, and 20-μL aliquots were analyzed by liquid scintillation counting. The first labeled peak contains sugars and *O*-glycosides which elute well before inosine (5 and 8 min, respectively). The peak containing sugars and glycosides was pooled and concentrated under reduced pressure. The peak was loaded on a Dowex 50-X8 column in the Ca^{2+} form (1.5 × 42.9 cm) and eluted with distilled water. This chromatography system separates sugars from their *O*-glycosides (Angyal et al., 1979). Fractions of 5.5 mL were collected, and 1-mL aliquots were analyzed by liquid scintillation counting.

Ribose Exchange Reaction. Reaction mixtures contained 50 mM triethanolamine hydrochloride, pH 7.5, 100 μM inosine containing 3 × 10^5 cpm [1′-^{3}H]inosine, 20 mM ribose, and 20 μM purine nucleoside phosphorylase in a volume of 1.0 mL. The mixture was incubated for 10 min at 30 °C, sufficient for a single hydrolytic turnover. A

Table 1: Comparison of Kinetic Isotope Effects for the Arsenolysis and Hydrolysis of Inosine by Purine Nucleoside Phosphorylase and Nucleoside Hydrolase

substrates	purine nucleoside phosphorylase pre-steady-state inosine hydrolysis kinetic isotope effect	purine nucleoside phosphorylase pre-steady-state inosine arsenolysis kinetic isotope effect[c]	nucleoside hydrolase steady-state kinetic isotope effects[d]	isotope and type of effect
[1′-^{3}H]inosine + [5′-^{14}C]inosine	1.151 ± 0.004 (6)[a] [1.129 ± 0.006 (3)][b]	1.141 ± 0.004	1.150 ± 0.006	1′-^{3}H, α-secondary
[2′-^{3}H]inosine + [5′-^{14}C]inosine	1.145 ± 0.003 (6)	1.152 ± 0.003	1.161 ± 0.003	2′-^{3}H, β-secondary
[1′-^{14}C]inosine + [5′-^{3}H]inosine	1.045 ± 0.005 (6)	1.026 ± 0.006	1.044 ± 0.004	1′-^{14}C, primary
[9-^{15}N,5′-^{14}C]inosine + [5′-^{3}H]inosine	1.000 ± 0.005 (6)	1.010 ± 0.005	1.026 ± 0.004	9-^{15}N, primary
[4′-^{3}H]inosine + [5′-^{14}C]inosine	1.006 ± 0.004 (3)	1.008 ± 0.004	0.992 ± 0.003	4′-^{3}H, γ-secondary
[5′-^{3}H]inosine + [5′-^{14}C]inosine	1.028 ± 0.005 (6)	1.033 ± 0.005	1.051 ± 0.003	5′-^{3}H, γ-secondary

[a] The numbers in parentheses are the number of samples analyzed to determine the kinetic isotope effect. The pre-steady-state kinetic isotope effects are corrected for the extent of substrate hydrolysis using eq 2. Enzyme and excess labeled substrate were incubated for 10 min to yield the enzyme−hypoxanthine complex, ribose, and unreacted inosine. At this time, 1.0 ± 0.1 mol of products is formed per mole of purine nucleoside phosphorylase trimer. Following acid treatment to stop the reaction, the ^{3}H/^{14}C ratio in product ribose is compared to that of the substrate inosine following its conversion to ribose as described in methods. Experiments which used [5′-^{3}H]inosine as the label for the isotopically insensitive position were corrected by the expression (observed isotope effect × 1.028). [b] Kinetic isotope effect for the steady-state (10 turnovers) hydrolytic reaction for purine nucleoside phosphorylase. Enzyme and excess labeled inosine were incubated for 6 h to achieve 10 turnovers. During this period, the trimeric purine nucleoside phosphorylase achieves a steady state with one tightly bound hypoxanthine (Kline & Schramm, 1992). The reaction is limited by the rate of hypoxanthine release. [c] Intrinsic kinetic isotope effect for arsenolysis taken from Kline and Schramm (1993). [d] Data taken from Horenstein et al. (1991).

sample (50 μL) was analyzed by HPLC and the area under the peaks analyzed for hypoxanthine and inosine content. The radioactivity present in the inosine and ribose peaks was determined by scintillation counting.

Transition-State Modeling. Transition states were defined by a combination of vibrational and semiempirical calculations as previously described (Mentch et al., 1987; Horenstein et al., 1991; Horenstein & Schramm, 1993a). Kinetic isotope effects were calculated from the transition-state geometries using the BEBOVIB-IV program (Quantum Chemistry Exchange Program No. 337; Sims et al., 1977). The reactant state was taken from the crystal structure of inosine (Munns & Tollin, 1970). The geometry of the ribose ring at the transition state was based on the crystal structure of ribonolactone, which shares sp^2 hybridization at C1 (Kinoshita et al., 1981). The incoming water nucleophile was modeled as an oxygen atom 180° from the breaking C1′−N9 bond. Because of the limitations on the number of atoms that can be used in BEBOVIB, a cutoff model of inosine was used which included all carbons and nitrogens of the ribosyl and imidazole portions of inosine as well as all other atoms α and β to the C−N glycosidic bond. The reaction coordinate was generated by coupling the stretching motion of the C1′−N9 bond with the forming C1′−O bond from the attacking oxygen. An interaction constant of 1.1 was used. Force constants were obtained from published sources (Wilson et al., 1955; Sims & Fry, 1974; Sims & Lewis, 1984). Alterations in bond lengths, bond angles, and the geometry of bonds distributed around C1′ were varied systematically with the extent of C1′−N9 bond breaking (Mentch et al., 1987; Horenstein et al., 1991; Kline & Schramm, 1993).

Molecular Electrostatic Potential Surfaces. The transition-state geometries determined from kinetic isotope effects and BEBOVIB-IV calculations were restored to complete molecular structure by addition of all atoms while retaining bond angles and lengths defined by the kinetic isotope effects. Bond lengths and angles other than those defining the transition state were optimized by MOPAC calculations (Coolidge & Stewart, 1990). The wave functions for the molecules were calculated using the STO-3G basis set in Gaussian 92 (Frisch et al., 1992). The Gaussian output was used in the AVS Chem Viewer routines to assign colors to regions of various electrostatic potential. Details of the molecular electrostatic potential surface analysis for enzymatic reactions have been published (Horenstein & Schramm, 1993a,b) and reviewed (Schramm et al., 1994).

RESULTS

Adenosine Is Not a Significant Substrate for Purine Nucleoside Phosphorylase. Adenosine is a substrate for purine nucleoside phosphorylase isolated from *Escherichia coli* and has been used as a slow substrate for kinetic isotope effect experiments with the mammalian enzyme (Stein et al., 1978; Stein & Cordes, 1981). A recent report indicated that adenosine is not a substrate for either the human or calf spleen purine nucleoside phosphorylase (Bzowska et al., 1990). Reaction mixtures were prepared with (*R*)-coformycin at a concentration (10 μM) which inhibits adenosine deaminase activity but does not inhibit purine nucleoside phosphorylase. No adenine or hypoxanthine could be detected in a reaction mixture which contained coformycin, while 1% of the adenosine was converted to hypoxanthine in a reaction mixture without coformycin. The results establish that calf spleen purine nucleoside phosphorylase hydrolyzes inosine at a rate at least 10^5 times greater than that for hydrolysis of adenosine. Commercial preparations of calf spleen nucleoside phosphorylase contain adenosine deaminase as a significant impurity (0.01−0.1%).

Kinetic Isotope Effects. The hydrolysis of inosine by purine nucleoside phosphorylase is sufficiently slow to obtain single turnover data without using rapid quench techniques. The observed kinetic isotope effects for single-turnover hydrolysis of inosine by purine nucleoside phosphorylase are listed in Table 1. The α- and β-secondary ^{3}H isotope effects of 1.151 and 1.145 at H1′ and H2′ are indicative of a well-developed oxocarbenium ion with nearly complete sp^2 hybridization at C1′. The large isotope effect at H2′ is indicative of hyperconjugation which occurs between C2′−H2′ and C1′−N9 when the orbital overlap is favorable for these bonds (Sunko et al., 1977; Schramm, 1991). The

γ-secondary ^3H kinetic isotope effect of 1.028 for the 5′-^3H position is highly significant and indicates altered bond order to this atom around C5′ at the transition state. The bonding changes at 4′-H are small, normal effects, suggesting minimal change for the C4′−H4′ bond at the transition state.

The [1′-^{14}C]inosine kinetic isotope effect of 1.045 is large for a dissociative mechanism and indicates that reaction coordinate motion for C1′ at the transition state is well developed and that C1′−N9 bond breaking is advanced. In contrast, the kinetic isotope effect with [9-^{15}N]inosine was insignificant. To ensure the validity of the 9-^{15}N primary isotope effect, the same mixture of [9-^{15}N,5′-^{14}C]inosine and [5′-^3H]inosine used for the hydrolysis of inosine by purine nucleoside phosphorylase was used to measure the 9-^{15}N kinetic isotope effect for nucleoside hydrolase. The value was 1.024 ± 0.004, in good agreement with the value of 1.026 ± 0.004 reported earlier with a different preparation of the labeled nucleosides [Table 1 and Horenstein et al. (1991)].

A kinetic isotope effect of 1.129 ± 0.006 was observed for [1′-^3H]inosine during multiple catalytic turnovers of the hydrolytic reaction. The slightly smaller isotope effect for the steady-state hydrolytic reaction represents an increased degree of internal commitment which reduces the kinetic isotope effect observed for the single-turnover reaction (see Discussion).

Equilibrium Isotope Effect. Hydrolysis of inosine by purine nucleoside phosphorylase is irreversible under the experimental conditions used for the kinetic isotope effect experiments. The equilibrium isotope effect can be estimated from the phosphorolysis of inosine since the bonding of ribose 1-PO_4 is similar in the C1′−O bond which is also sp^3 hybridized. The isotope effect in two experiments (six measurements) gave an average [1′-^3H] equilibrium isotope effect of 1.000 ± 0.009. All individual values were within 2% of unity.

Commitment to Catalysis. Catalytic commitment defines the probability with which enzyme-bound substrate is converted to products relative to release as unchanged substrate. This is expressed as k_3/k_2 for the hydrolytic reaction in eq 3. The catalytic commitment of bound inosine

$$E + \text{inosine} \overset{k_2}{\leftarrow} E\cdot\text{inosine} \overset{k_3}{\rightarrow} E + \text{hypoxanthine} + \text{ribose} \quad (3)$$

was measured using the pulse−chase method of Rose (1980). Sufficient labeled inosine was added to convert 98% of enzyme to the E·inosine complex. Addition of a large excess of unlabeled inosine at 10 s, prior to the first catalytic turnover, allows partitioning of the E·inosine complex during the subsequent 5−10 turnovers without rebinding of labeled inosine. Under these conditions, there was no detectable formation of labeled products. Thus $k_2 \gg k_3$ for the hydrolytic reaction. Under the experimental conditions, a commitment of 0.02 could have been detected, provided that the E·inosine complex is formed in 10 s and that the E·inosine binary complex formed under these conditions is catalytically competent. These provisos were tested directly by commitment experiments using the phosphorolysis reaction.

Commitment to catalysis for the phosphorolysis of inosine was accomplished as described above except that phosphate was also present with the addition of excess unlabeled inosine. Under these conditions, the commitment of bound inosine to catalysis was a function of phosphate concentration as shown in Figure 2. When phosphate was extrapolated to a saturating concentration, 20.4 ± 3.3 μM inosine was trapped and converted to products from a purine nucleoside phosphorylase concentration of 30 μM. The forward commitment factor for phosphorolysis was 2.1 for the E·inosine complex. During phosphorolysis of inosine, k_3/k_2 of eq 3 also includes phosphate binding and ribose 1-phosphate release in the k_3 step. The result establishes that the 10-s incubation is sufficient time to form the E·inosine complex, that the E·inosine complex is catalytically competent, and that, for phosphorolysis, the forward commitment is large.

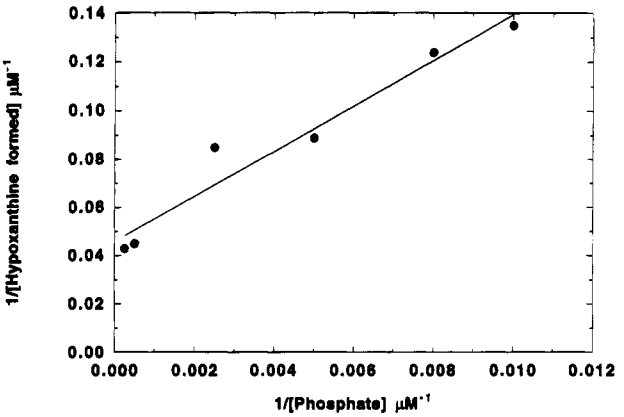

FIGURE 2: Commitment to phosphorolysis of enzyme-bound inosine. A Michaelis complex of 30 μM purine nucleoside phosphorylase (as trimer) with bound [8-^{14}C]inosine was diluted 50-fold with buffered 5 mM inosine containing variable phosphate concentrations as shown in the figure. The amount of bound inosine converted to product is plotted on the ordinate. The line was fit by linear least squares analysis. The ordinate intercept gave a value of 20.4 ± 3.3 μM [8-^{14}C]hypoxanthine formed, and the slope indicates an apparent dissociation constant of 203 ± 39 μM for inorganic phosphate.

Methanolysis of Inosine during the Hydrolytic Reaction. Hydrolysis of inosine by purine nucleoside phosphorylase in solvent containing 20% methanol was used to determine if methanol can serve as a nucleophile in competition with H_2O. The reaction conditions produced a single catalytic turnover. Unreacted [1′-^3H]inosine, [1′-^3H]ribose, and 1-methyl[1-^3H]ribose were resolved by HPLC and Dowex chromatography. The fraction of inosine converted to products confirmed that a single turnover had occurred. The elution profile of ribose and 1-methylribose is shown in Figure 3. Approximately 85% of the product is 1-methylribose, indicating that the transition-state complex is susceptible to attack by solvent nucleophiles.

External Reversibility of Ribose Hydrolysis. Hypoxanthine release is the rate-limiting step for inosine hydrolysis, with the more rapid release of ribose in an earlier step (Kline & Schramm, 1992). The reversibility of inosine formation following ribose release from the tightly bound enzyme−hypoxanthine was tested by measuring a single turnover reaction with [1′-^3H]inosine in the presence of excess unlabeled ribose. Hydrolysis of [1′-^3H]inosine would cause release of [1-^3H]ribose in the direction of hydrolysis. Rebinding of unlabeled ribose (present in 1000-fold molar excess of enzyme) to the enzyme−hypoxanthine complex could then result in the formation and release of unlabeled inosine. Thus, internal exchange of [1-^3H]ribose for unlabeled ribose would be accompanied by loss of specific radioactivity from [1′-^3H]inosine following the first complete

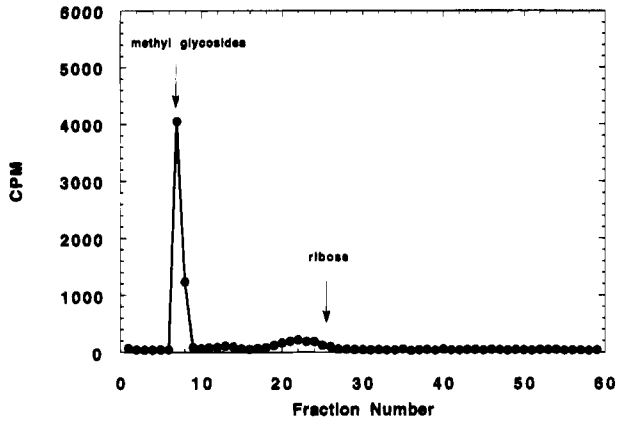

FIGURE 3: Conversion of [1′-^{3}H]inosine to 1-methyl[1-^{3}H]ribose and [1-^{3}H]ribose during single-turnover kinetics in the presence of methanol. Solvolysis was accomplished with purine nucleoside phosphorylase in 20% (by volume) methanol. HPLC was used to resolve ribose and methyl ribosides from inosine and hypoxanthine. The sugars were resolved on Dowex 50-X8, Ca^{2+} form. The column was calibrated using D-ribose and a mixture of methyl α- and β-D-ribosides; the elution positions are shown by the arrows.

turnover. These steps are summarized in eq 4. In a reaction

$$\begin{matrix} \text{E·[1′-}^3\text{H]inosine} \rightleftarrows \text{E·hypoxanthine} \rightleftarrows \\ \quad + \text{ribose} \qquad\qquad \text{·[1-}^3\text{H]ribose} \\ \qquad\qquad\qquad\qquad + \text{ribose} \end{matrix}$$

$$\begin{matrix} \text{E·hypoxanthine} \xrightarrow{\text{slow}} \text{E} + \text{hypoxanthine} \\ + \text{[1-}^3\text{H]ribose} \\ \quad + \text{ribose} \end{matrix} \quad (4)$$

which allowed one turnover of [1′-^{3}H]inosine to E·hypoxanthine and free [1-^{3}H]ribose, there was no exchange of unlabeled ribose into [1′-^{3}H]inosine (Table 2). Thus, ribose cannot rebind to the enzyme–hypoxanthine complex and return to inosine during single-turnover kinetics.

DISCUSSION

Kinetic Steps in the Hydrolytic Reaction. Hydrolysis of inosine by purine nucleoside phosphorylase is characterized by C1′–N9 bond cleavage, release of ribose, and the formation of a tightly bound complex with hypoxanthine and reaction at only one of the three catalytic sites of this trimeric enzyme (Kline & Schramm, 1992). The hydrolytic reaction is 4 orders of magnitude slower than the arsenolysis or phosphorolysis reactions, but both hydrolytic and arsenolysis reactions show a single-turnover burst of product followed by a slower steady state in which steps related to hypoxanthine release are rate-limiting (Kline & Schramm, 1993). The enzyme–hypoxanthine complex has a dissociation constant

Table 2: Products from [1′-^{3}H]Inosine during Single-Turnover Hydrolysis in the Presence of Excess Ribose[a]

before enzyme	nmol	specific radioactivity, cpm/nmol
[1′-^{3}H]inosine	100	300

after one turnover[b]	nmol (UV analysis)	nmol (^{3}H counting)	specific radioactivity, cpm/nmol
[1′-^{3}H]inosine	77	79	308
hypoxanthine	23		
[1-^{3}H]ribose		21	276[c]

[a] Unlabeled ribose was present at 20 mM (20 000 nmol), and the enzyme was present at 20 nmol. [b] A single hydrolytic turnover occurred in 10 min. The products were resolved on HPLC and analyzed by ultraviolet spectrophotometry and scintillation counting as described in Methods. [c] Calculated from ([1-^{3}H]ribose/hypoxanthine) × 300.

of 1.3×10^{-12} M when formed in the hydrolytic reaction and can be directly isolated by gel filtration as a noncovalent, stoichiometric complex. Equilibrium dialysis of enzyme and hypoxanthine in the presence of phosphate gives three hypoxanthines bound per trimer and a dissociation constant of 1.6 μM, establishing that the tightly bound complex is a consequence of the hydrolytic reaction, which must therefore isomerize to permit hypoxanthine release. These steps are summarized in Scheme 1. The slow hydrolytic reaction establishes that the enzyme is capable of reaching the hydrolytic transition state without participation of a phosphate or arsenate anion. Quantitation of the hydrolytic reaction allows the determination of the role of the nucleophile in catalysis and transition-state stabilization.

Nature of the Hydrolytic Reaction Complex. Several nucleoside and nucleotide *N*-glycohydrolases, including AMP nucleosidase and nucleoside hydrolase, contain a specific water nucleophile which is enzymatically activated and cannot be replaced by other solvent nucleophiles including methanol (Parkin & Schramm, 1987; Mentch et al., 1987; Horenstein et al., 1991). Arsenolysis of inosine by purine nucleoside phosphorylase is also specific, excluding both solvent water and methanol (Kline & Schramm, 1992). Solvolysis of inosine in the presence of 20% methanol resulted in production of approximately 85% of the ribose product as 1-methylribose. Similar results have been found with NAD^+ glycohydrolase in the presence of methanol (Schuber et al., 1976). Methanolysis occurs in hydrolytic reactions when the enzyme destablizes the substrate to create a reactive species which is accessible to solvent and therefore susceptible to attack by solvent nucleophiles according to the relative nucleophilicity. Departure from this ratio indicates a preference of the catalytic pocket for specific

Scheme 1: Constants Describing the Hydrolysis of Inosine by Purine Nucleoside Phosphorylase[a]

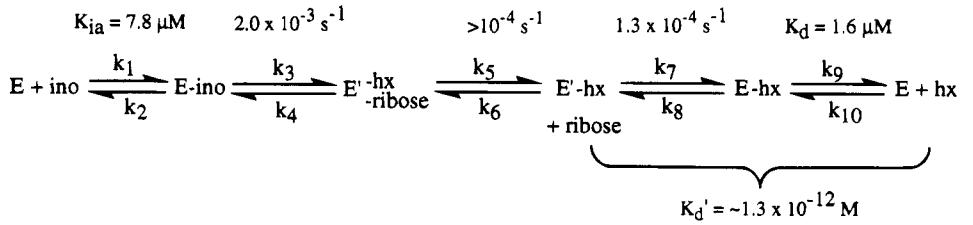

[a] The purine nucleoside phosphorylase trimer is E, and ino represents the single inosine which binds productively to the enzyme, followed by its hydrolysis to hypoxanthine (hx). Although not indicated in the reaction, binding of E to hx occurs uniformly at all three subunits. The data are from Kline and Schramm (1992).

solvent nucleophiles. Methanol is estimated to be a factor of 10^2 more nucleophilic than water (Jencks, 1969), and at 20% by volume, the molecular ratio of H_2O to methanol is 10:1. The expected partition would thus be 91% methanolysis, in good agreement with the observed formation of 85% 1-methylribose. The enzyme develops an unstable transition state which permits the attack of solvent nucleophiles. No preference is demonstrated for H_2O, suggesting free solvent access to the anomeric carbon at the transition state. The X-ray crystal structure of the human erythrocyte enzyme suggests that a peptide loop closes over the phosphate region, making close contacts (Ealick et al., 1990). Without phosphate, the flap may remain sufficiently open to permit free access to solvent, although the reaction rate is slow without the protein-enforced participation of the anionic nucleophile.

Phosphate enhances the probability that bound inosine will react, resulting in the large commitment factor. The commitment is consistent with the small kinetic isotope effects observed for the phosphorolysis reaction of purine nucleoside phosphorylase (Kline & Schramm, 1993). When the observed kinetic isotope effect of 1.047 ± 0.002 for the phosphorolysis reaction is corrected for the forward commitment of 2.1, the intrinsic [1′-^{3}H]inosine kinetic isotope effect for phosphorolysis is approximately 1.14, which is the same as that observed for arsenolysis and near the value of 1.151 observed for hydrolysis. The transition-state structure for arsenolysis is thus similar to that for phosphorolysis.

Kinetic Isotope Effects for the Hydrolytic Reaction. Kinetic isotope effects are diagnostic for the nature of the transition state in reactions where bond-breaking is the highest barrier on the reaction coordinate and where commitment factors are negligible (Hogg et al., 1980; Northrop, 1981; Fry, 1964; Schramm et al., 1994). Bound inosine is uncommitted to catalysis in the hydrolytic reaction of purine nucleoside phosphorylase, and the kinetic isotope effects (except for 9-^{15}N) are similar to those observed for similar reactions which are known to express kinetic isotope effects and to exhibit transition states with oxocarbenium character (Table 1). It can be concluded that the transition state for the hydrolytic reaction of purine nucleoside hydrolase contains oxocarbenium character with open access to solvent molecules because of the missing anion and possibly because of an inability of the enzyme to close the anion flap. The slow catalytic rate and the open architecture of the catalytic site permit facile escape of bound inosine prior to catalysis.

An exception to the similarity of kinetic isotope effects for the arsenolysis and hydrolytic reactions of purine nucleoside phosphorylase is that from [9-^{15}N]inosine. It was not possible to identify a chemically reasonable transition state which included the well-established oxocarbenium character but gave rise to an insignificant 9-^{15}N isotope effect. Specific suppression of the ^{15}N isotope effect would occur by an internal reversal of *N*-glycosidic bond hydrolysis from bound hypoxanthine and ribose which leads to the formation of inosine. This sequence can occur only from bound ribose, since exchange of external ribose to inosine does not occur during hydrolysis. In this mechanism, the observed kinetic isotope effects for ^{15}N are most affected since the equilibrium isotope effects for the conversion of inosine to ribose are relatively small for isotopic substitutions in the sugar, while those for the conversion of [9-^{15}N]inosine to bound

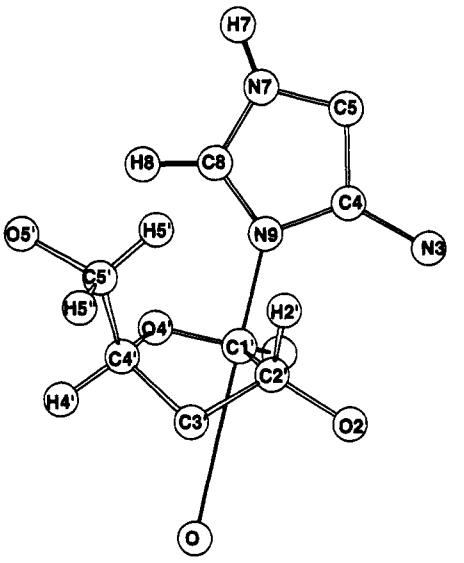

Bond	Reactant Bond Length Å	Transition State Bond Length Å
C1'-N9	1.47	1.90 ± 0.12
C1'-O4'	1.42	1.32 ± 0.06
C1'-H1'	1.13	1.12 ± 0.001
C1'-O		2.96 ± 0.4
C1'-C2'	1.53	1.50 ± 0.003
C2'-H2'	1.12	1.16 ± 0.002
N9-C8	1.37	1.33 ± 0.005
N9-C4	1.37	1.39 ± 0.004
C8-N7	1.31	1.34 ± 0.003

FIGURE 4: Transition-state geometry for the hydrolytic reaction catalyzed by purine nucleoside phosphorylase. The structure was determined by a comparison of the kinetic isotope effects (Table 1) with those computed for systematically varied transition-state geometries using bond-vibrational analysis (Sims & Lewis, 1984). The observed 9-^{15}N primary isotope effect was corrected for the equilibrium isotope effect on protonation of ^{15}N (see Discussion). The attacking water nucleophile is shown as an oxygen with low bond order to C1′. Protonation of N7, rehybridization of C1′ to near sp^2 geometry, and a C3′-*exo* ribosyl ring pucker are distinguishing features of the transition state. These can be compared to substrate in Figure 5. Bond lengths in the transition state are assigned limits based on the accuracy of the kinetic isotope effects which establish the indicated bond. The C1′−N9 bond length is determined from the ^{15}N9, ^{14}C1′, and ^{3}H1′ isotope effects. For example, in an S_N2 mechanism where both C1′−N9 and C1′−O exhibit substantial bonding in the transition state, the ^{14}C1′ kinetic isotope is large (1.12), and ^{3}H1′ and ^{3}H2′ are both expected to be near 1.00. These relationships are discussed in more detail in Mentch et al. (1987) and Horenstein et al. (1991) and especially in Sims and Lewis (1984) and Huskey (1991). The bond lengths for reactant inosine were taken from the X-ray crystal structure or from inosine structures with geometries optimized by MOPAC calculations to define bonds to hydrogen.

N9-protonated hypoxanthine are not. The equilibrium ^{15}N-isotope effect for the conversion of inosine to N9-protonated hypoxanthine was calculated to be 0.978 using BEBOVIB-IV calculations for the two structures. Since the observed 9-^{15}N isotope effect of 1.000 is the product of the forward and the equilibrium effects, the intrinsic 9-^{15}N isotope effect for transition-state formation is near 1.022. This value can be seen to be in close agreement with other reactions of similar chemistry (Table 1). In contrast, the 1′-^{3}H equilibrium isotope effects calculated for the inosine−ribose pair are small relative to the kinetic isotope effect, approximately 1.025 depending on the C1−H1 bond length assignment for

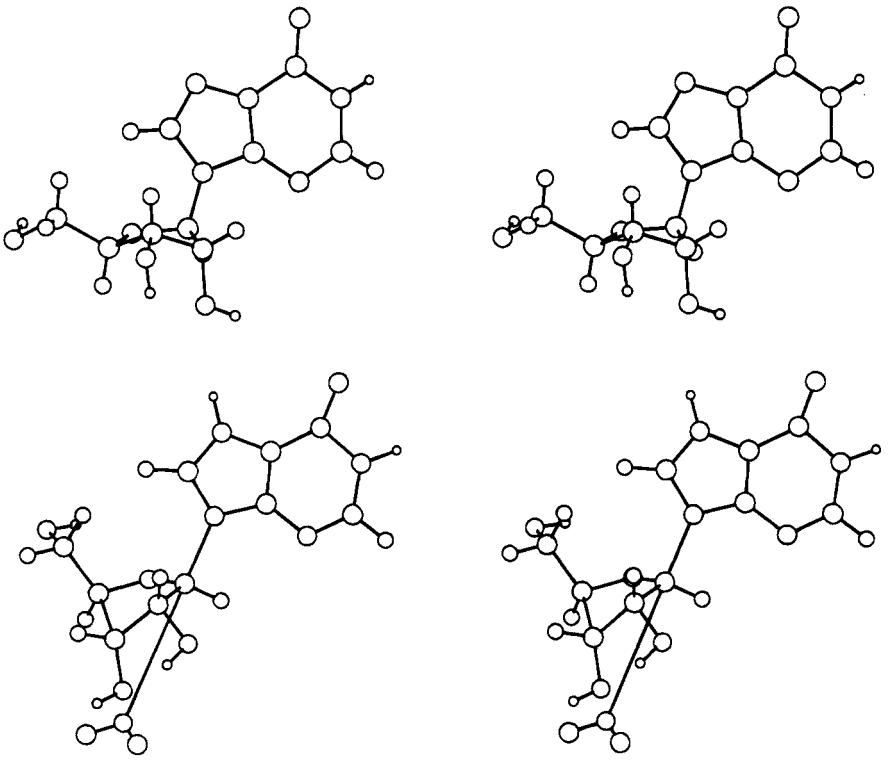

FIGURE 5: Stereoviews of the substrate inosine (upper panel) and the transition state (lower panel). The C1′−N9 bond has lengthened from 1.48 to 1.90 Å, the attacking nucleophile has just begun its attack at 2.96 Å, and the C1′−O4′ bond has shortened to 1.32 Å. The conformation of the ribose ring has changed from C3′-*endo* to C3′-*exo*, and N7 is protonated.

ribose. *Ab initio* calculations on the related model compound, 2-deoxy-β-D-glycerotetrofuranose, gave C1−H1 bond lengths of 1.085 to 1.108 depending on basis set and pseudorotational geometry (Garrett & Serianni, 1990); thus the exact equilibrium isotope effect will be small, but is difficult to assign. Experimental determination of the 1′-^{3}H equilibrium effect for phosphorolysis is consistent with these calculations and gave values within 2% of unity, in concert with previous measurements and estimates for the equilibrium isotope effect using the *E. coli* enzyme (Sinnott & Krenitsky, 1989; Guo et al., 1991).

The remote kinetic isotope effect of 1.028 from [5′-^{3}H]-inosine requires that the C5′ hybridization be altered in the transition state (Horenstein & Schramm, 1993a; Kline & Schramm, 1993). The X-ray crystal structure of purine nucleoside phosphorylase shows His257 hydrogen-bonded to the hydroxyl of C5′ (see below). Model calculations demonstrate that a normal-energy hydrogen bond to the C5′-hydroxyl provides sufficient distortion at C5′ to cause up to a 5% normal ^{3}H kinetic isotope effect at this position (Horenstein et al., 1991). Normal mode analysis reveals that the isotope effect is due primarily to altered out-of-plane bending, which is not reflected in a significant ^{14}C effect due to the increased mass of carbon. The 5′-^{3}H isotope effect for the related enzyme, nucleoside hydrolase, is 1.051 (Table 1). Evidence for its involvement in transition-state formation is evident since the 5′-deoxynucleosides are catalytically inert. The observation of a significant [5′-^{3}H]inosine kinetic isotope effect for both arsenolysis and hydrolysis reactions implicates this group in transition-state anchoring for both reactions of purine nucleoside phosphorylase.

Reaction Coordinate. The features of the reaction coordinate must include freely reversible inosine binding since no forward commitment occurs. Thus the chemical step (k_3 in Scheme 1) is slow compared to substrate addition (k_1) and release (k_2). A subsequent step completely obscures the ^{15}N effect while allowing full expression of the ^{14}C and ^{3}H effects from the ribose. Internal chemical equilibrium occurs by k_4 because of slow release of ribose (k_5). Failure of external ribose to exchange into inosine establishes that ribose binding is poor or that a step between ribose addition and inosine release is unfavorable relative to the hypoxanthine release. Since hypoxanthine release is the slowest step of the reaction cycle, ribose rebinding does not occur to a significant extent at 20 mM ribose. Release of hypoxanthine is predicated on an enzyme isomerization (k_7) which is the largest energy barrier during hydrolysis (Kline & Schramm, 1992). This noncovalent complex has an apparent K_d of 1.3 × 10^{-12} M and has been isolated. Following k_7, E•hypoxanthine binding is weakened by 6 orders of magnitude to 1.6 μM. Steps k_7-k_{10} are reversible, since incubation of enzyme with excess hypoxanthine permits formation of E′•hx (Kline & Schramm, 1992).

The observed kinetic isotope effects are thus the product of the kinetic and equilibrium isotope effects between free inosine and enzyme-bound hypoxanthine and ribose. The observed ^{15}N isotope effect is influenced because of the inverse isotope effect of ^{15}N9 protonation, but the equilibrium isotope effects for conversion of inosine to ribose are small since C1′ remains sp^3-hybridized in both states and the C1′−N9 glycosidic bond of inosine is replaced by a vibrationally similar C1′−O bond in ribose. A slightly smaller 1′-^{3}H kinetic isotope effect was observed for multiple turnovers than for the single-turnover reaction. If release of ribose resulted in a small inverse isotope effect which is not fully observed in the single-turnover reaction, because of incomplete ribose release, the result could be explained. However, the physical basis for this observation is not well established.

Transition-State Analysis. Using the kinetic isotope effects observed for the isotopic labels in ribose and the value of 1.022 deduced for the 9-^{15}N isotope effect, kinetic isotope effects for specific models of the transition state were determined by bond-energy bond-order vibrational analysis and compared to the experimental kinetic isotope effects from Table 1. The bond lengths of reactant inosine and the transition-state structure are summarized in Figure 4, and the results of the analysis are provided as stereo diagrams of the substrate and transition state in Figure 5. The experimental kinetic isotope effects could only be fit to transition-state structures closely related to that of Figure 4. The features of the transition state include a bond length of 1.90 Å in the *N*-ribosidic bond and 2.96 Å to the attacking water nucleophile. The loss of bond order to C1′ at the transition state causes the carbon to rehybridize to sp^2, causing an altered pucker in the ribose ring to 3′-*exo*, compared to the 3′-*endo* pucker of inosine.

Kinetic isotope effects from nucleoside hydrolase (Table 1) are similar to those for the hydrolytic reaction of purine nucleoside phosphorylase, except for the 9-^{15}N primary effect, caused by the reverse commitment, and the γ-secondary 4′-^{3}H and 5′-^{3}H effects caused by small bond-order changes due to enzyme-specific contacts with the 5′-methoxy group of nucleosides. The 5′-hydroxymethyl contacts are predicted in the crystal structure of purine nucleoside phosphorylase and involve normal hydrogen bonds between His257 and the 5′-hydroxyl of the nucleoside (Ealick et al., 1991). The smaller isotope effects observed with purine nucleoside phosphorylase establish that the distortion at the C5′ position is less than that experienced at the transition state of nucleoside hydrolase (Horenstein et al., 1991; Horenstein & Schramm, 1993a).

Comparison of Hydrolytic and Arsenolytic Transition States. Arsenolysis of inosine by purine nucleoside phosphorylase is characterized by a transition state with an N9−C1′ bond of 1.77 Å compared to that of 1.90 Å for the hydrolytic reaction. Thus, the hydrolytic transition state occurs later in the reaction coordinate. Filling the anionic site with AsO_4 provides an enzyme-directed nucleophile which lowers the transition-state barrier to increase the reaction rate by 1.5×10^4 (Kline & Schramm, 1992). As the oxocarbenium is formed by the enzyme, it is efficiently captured by PO_4 or AsO_4 anions as preassociated incipient nucleophiles. Without anions, the anionic binding site is filled with undirected solvent molecules which attack C1′ as the enzyme destabilizes the N9−C1′ bond. The X-ray crystal structure of the human erythrocyte purine nucleoside phosphorylase shows a hydrophobic patch for hypoxanthine binding, a hydrogen bond network at the anionic site, but remarkably few interactions capable of stabilizing an oxocarbenium ion (Ealick et al., 1991). Participation of the incipient nucleophile at the transition state is similar for arsenolysis and hydrolysis with C1′-O bonds of 3.01 and 2.96 Å, respectively. However, the entropy of an immobilized anion will be substantially lower than the equivalent volume occupied by a group of thermally excited solvent molecules.

Molecular Electrostatic Potential Surfaces for Inosine, Hydrolytic, and Arsenolysis Transition States. Electrostatic potential surfaces for inosine and transition-state structures of inosine with and without preassociated nucleophiles are shown in Figure 6. The transition-state structures show

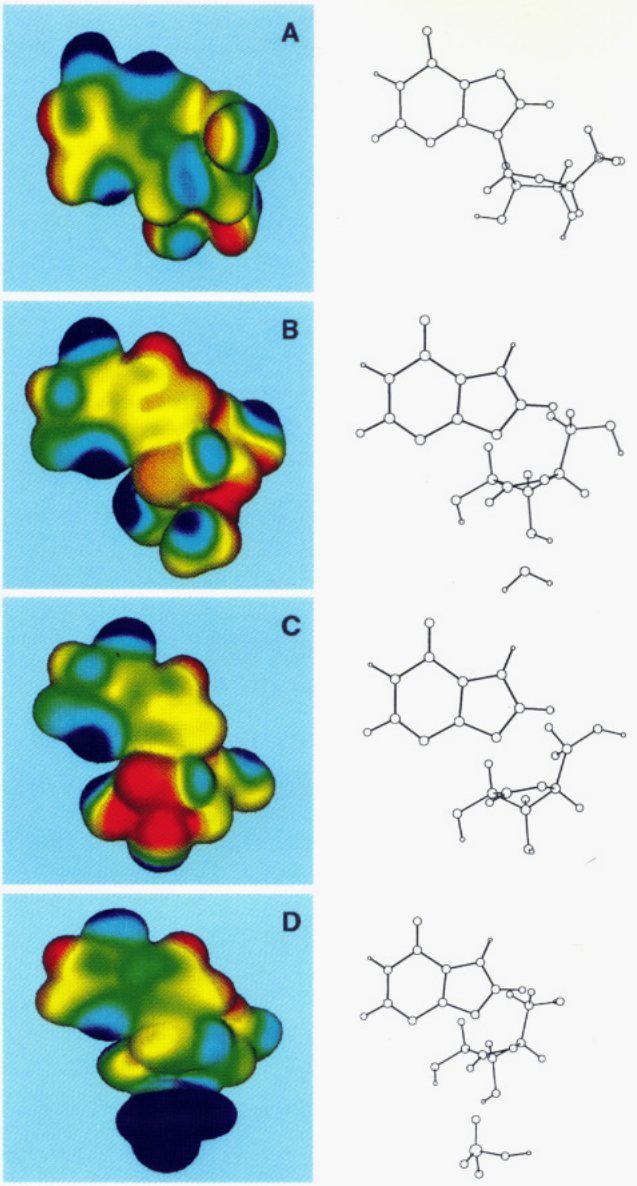

FIGURE 6: Molecular electrostatic potential surfaces for purine nucleoside phosphorylase: (A) inosine; (B) transition state for the hydrolytic reaction catalyzed by purine nucleoside phosphorylase; (C) transition state without the preassociated water nucleophile; (D) transition-state structure for the arsenolysis reaction of inosine with purine nucleoside phosphorylase. The molecular electrostatic surfaces use blue to represent negative electrostatic potential (partial negative charge) and red to represent positive electrostatic potential (partial positive charge). The stick figures to the right show the location of the atoms in the same orientation as in panels A−D. In panels B and D, the attacking H_2O and arsenate nucleophiles are shown below C1′ at their respective locations in the transition state.

regions of partial charge and the relative volumes occupied by water and arsenate nucleophiles. Without a nucleophile present, the relatively highly charged oxocarbenium formed from the ribose ring is clearly seen. Jencks (1980) has discussed the role of preassociated nucleophiles in carbocationic mechanisms, with the conclusion that the nucleophile plays an important role in permitting formation of the transition state. The same conclusion can be drawn from the transition states for hydrolysis and arsenolysis of inosine. As the nucleophile becomes better, the transition state is formed earlier in the reaction coordinate and the reaction rate increases by 10^4. The volume occupied by arsenate is substantial, easily large enough to occupy a water or

methanol molecule. A major effect of the anion is to neutralize the carbocation. Arsenate, located at the transition-state position, completely neutralizes the partial positive charge at the transition state (Figures 6C,D). In contrast, water at the transition state neutralizes a smaller portion of the charge (Figure 6B,C).

CONCLUSIONS

Multiple kinetic and equilibrium isotope effects for the hydrolytic reaction of purine nucleoside phosphorylase established a transition state which shares many of the features seen for other purine *N*-glycohydrolases. The transition state contains substantial oxocarbenium ion character, and the conformation of the ribose ring is C3′-*exo* as determined from the H2′ kinetic isotope effects. The observed 9-^{15}N kinetic isotope effect is influenced by reversible formation of the *N*-glycosidic bond prior to ribose release. The transition state allows unhindered approach of solvent nucleophiles. The role of the incipient nucleophilic anion is to enforce an earlier transition state than for the hydrolytic reaction.

REFERENCES

Angyal, S. J., Bethell, G. S., & Beveridge, R. J. (1979) *Carbohydr. Res. 73*, 9−18.

Bigeleisen, J., & Wolfsberg, M. (1958) *Adv. Phys. Chem. 1*, 15−76.

Bzowska, A., Kulilowska, E., & Shugar, D. (1990) *Z. Naturforsch. 45C*, 59−70.

Coolidge, M. B., & Stewart, J. J. P. (1990) Quantum Chemistry Program Exchange, MOPAC 6.0, No. 455, Indiana University, Bloomington, IN.

Dahlquist, F. W., Rand-Meir, T., & Raftery, M. A. (1969) *Biochemistry 8*, 4214−4221.

Ealick, S. E., Rule, S. A., Carter, D. C., Greenhough, T. J., Babu, Y. S., Cook, W. J., Habash, J., Helliwell, J. R., Stoeckler, J. D., Parks, R. E., Jr., Chen, S., & Bugg, C. E. (1990) *J. Biol. Chem. 265*, 1812−1820.

Ealick, S. E., Babu, Y. S., Bugg, C. E., Erion, M. D., Guida, W. C., Montgomery, J.A., & Secrist, J. A., III (1991) *Proc. Natl. Acad. Sci. U.S.A. 88*, 11540−11544.

Frisch, M. J., Trucks, G. W., Head-Gordon, M., Gill, P. M. W., Wong, M. W., Foresman, J. B., Johnson, B. G., Schlegel, H. B., Robb, M. A., Replogle, E. S., Gomperts, R., Andres, J. L., Raghavachari, K., Binkley, J. S., Gonzalez, C., Martin, R. L., Fox, D. J., Defrees, D. J., Baker, J., Stewart, J. J. P., & Pople, J. A. (1992) Gaussian 92, revision E.3, Gaussian, Inc., Pittsburgh, PA.

Fry, A. (1964) *Pure Appl. Chem. 8*, 409−419.

Garrett, E. C., & Serianni, A. S. (1990) *Carbohydr. Res. 206*, 183−191.

Guo, X., Ashwell, M., Sinnott, M., & Krenitsky, T. A. (1991) *Biochem. J. 278*, 487−491.

Hogg, J. L., Rodgers, J., Kovach, I., & Schowen, R. L. (1980) *J. Am. Chem. Soc. 102*, 79−85.

Horenstein, B. A., & Schramm, V. L. (1993a) *Biochemistry 32*, 7089−7097.

Horenstein, B. A., & Schramm, V. L. (1993b) *Biochemistry 32*, 9917−9925.

Horenstein, B. A., Parkin, D. W., Estupiñán, B., & Schramm, V. L. (1991) *Biochemistry 30*, 10788−10795.

Huskey, W. P. (1991) in *Enzyme Mechanisms from Isotope Effects* (Cook, P. F., Ed.) pp 37−72, CRC Press Inc., Boca Raton, FL.

Jencks, W. P. (1969) *Catalysis in Chemistry and Enzymology*, pp 91−101, McGraw-Hill Book Co., Inc., New York.

Jencks, W. P. (1980) *Acc. Chem. Res. 13*, 161−169.

Kim, B. Y., Cha, S., & Parks, R. E., Jr. (1968) *J. Biol. Chem. 243*, 1771−1776.

Kinoshita, Y., Ruble, J. R., & Jeffrey, G. A. (1981) *Carbohydr. Res. 92*, 1−7.

Kline, P. C., & Schramm, V. L. (1992) *Biochemistry 31*, 5964−5973.

Kline, P. C., & Schramm, V. L. (1993) *Biochemistry 32*, 13212−13219.

Krenitsky, T. (1967) *Mol. Pharmacol. 3*, 526−536.

Mentch, F., Parkin, D. W., & Schramm, V. L. (1987) *Biochemistry 26*, 921−930.

Munns, A. R. I., & Tollin, P. (1970) *Acta Crystallogr., Sect. B 26*, 1101−1113.

Northrop, D. B. (1981) *Annu. Rev. Biochem. 50*, 103−131.

Parkin, D. W., & Schramm, V. L. (1987) *Biochemistry 26*, 913−920.

Parkin, D. W., Leung, H. B., & Schramm, V. L. (1984) *J. Biol. Chem. 259*, 9411−9417.

Parkin, D. W., Mentch, F., Banks, G. A., Horenstein, B. A., & Schramm, V. L. (1991) *Biochemistry 30*, 4586−4594.

Parks, R. E., Jr., & Agarwal, R. P. (1972) in *The Enzymes* (Boyer, P. D., Ed.) Vol. 7, pp 483−514, Academic Press, New York.

Porter, D. J. T. (1992) *J. Biol. Chem. 267*, 7342−7351.

Rose, I. A. (1980) *Methods Enzymol. 64*, 47−83.

Schramm, V. L. (1991) in *Enzyme Mechanism from Isotope Effects* (Cook, P. F., Ed.) pp 367−388, CRC Press, Boca Raton, FL.

Schramm, V. L., Horenstein, B. A., & Kline, P. C. (1994) *J. Biol. Chem. 269*, 18259−18262.

Schuber, F., Travo, P., & Pascal, M. (1976) *Eur. J. Biochem. 69*, 593−602.

Sims, L. B., & Fry, A. (1974) *Special Publication No. 1*, University of Arkansas, Fayetteville, AR.

Sims, L. B., & Lewis, D. E. (1984) *Isot. Org. Chem. 6*, 161−259.

Sims, L. B., Burton, G. W., & Lewis, D. E. (1977) *Quantum Chemistry Program Exchange*, No. 337, Indiana University, Bloomington, IN.

Sinnott, M., & Krenitsky, T. A. (1991) *Biochem. J. 257*, 355−359.

Stein, R. L., & Cordes, E. H. (1981) *J. Biol. Chem. 256*, 767−772.

Stein, R. L., Romero, R., Bull, H. G., & Cordes, E. H. (1978) *J. Am. Chem. Soc. 100*, 6249−6251.

Sunko, D. E., Szele, I., & Hehre, W. J. (1977) *J. Am. Chem. Soc. 99*, 5000−5002.

Wilson, E. B., Decius, J. C., & Cross, P. C. (1955) *Molecular Vibrations*, McGraw-Hill Book Co., Inc., New York.

BI941398C